

# **Magnesium & Fluorine Doped LMR-NMC Cathode Materials for High Energy Density Lithium-Ion Batteries**

A Project Report

Submitted to the Department of Chemistry  
Indian Institute of Technology Hyderabad  
In Partial Fulfillment of the Requirements for  
Degree of  
Master of Science

By

**Neha**

**Roll No. CY14MSCST11008**

*Under supervision of*

***Dr. Surendra Kumar Martha***



भारतीय प्रौद्योगिकी संस्थान हैदराबाद  
Indian Institute of Technology Hyderabad

Department of Chemistry  
Indian Institute of Technology Hyderabad  
April, 2016

## Declaration

I hereby declare that the matter embodied in this report is the result of investigation carried out by me in the Department of Chemistry, Indian Institute of Technology Hyderabad under the supervision of **Dr. Surendra Kumar Martha.**

In keeping with general practice of reporting scientific observations, due acknowledgement has been made wherever the work described is based on the findings of other investigators.



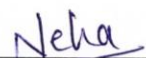
Signature of the Supervisor

**Dr. SURENDRA K. MARTHA**

Assistant Professor

Department of Chemistry

Indian Institute of Technology Hyderabad



(Signature)

Neha

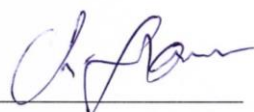
(Student Name)

CY14MSCST11008

(Roll No)

## Approval Sheet


This thesis entitled *Magnesium & Fluorine Doped LMR-NMC Cathode Materials for High Energy Density Lithium-Ion Batteries* by **Neha** is approved for the degree of Master of Science from IIT Hyderabad.



-Name and affiliation-  
Examiner



**Dr. M. Deepa** Name and affiliation-  
**Head & Associate Professor** Examiner  
**Department of Chemistry**  
Indian Institute of Technology Hyderabad



-Name and affiliation-  
Adviser

**Dr. SURENDRA K. MARTHA**  
**Assistant Professor**  
**Department of Chemistry**  
Indian Institute of Technology Hyderabad

## Acknowledgements

It gives me immense pleasure to express my profound gratitude to my project supervisor **Dr. Surendra Kumar Martha** for giving me an opportunity to work with him in his research group. I thank him all the time for his valuable guidance, encouragement and constant motivation during last one year. I will always remain grateful to him and consider myself privileged to be associated with him.

I wish to thank PhD scholar Mr. S. Krishna Kumar who contributed more significantly to this work, and also assisting, supporting, guiding me during the course of this research work.

I am highly thankful to other PhD students in our research group Mr. Naresh Vangapally, and Mr. Sourav Ghosh for their constant support throughout in learning various experimental techniques and conceptual understanding which has really helped me during the course of the project.

I sincerely thank Head of the Department (Dr. M. Deepa) and other faculty members of the Department of chemistry IIT Hyderabad for their constant encouragement during the course of study.

I express my sincere thanks to my family, friends and group members for their valuable presence and support.

Dedicated to  
***MY BELOVED PARENTS***  
&  
***MY RESPECTED TEACHERS***

# Contents

List of Figures .....	8
List of Tables .....	8
Abstract .....	9
<b>1 Introduction to Lithium Ion Battery (LIB) .....</b>	<b>11</b>
1.1 Motivation.....	11
1.2 Why LIB Among batteries.....	12
1.3 Introduction.....	12
1.3.1 Working Principle of LIB .....	14
1.3.2 Current Status of LIB.....	16
1.3.2(a) Anode Materials for LIB .....	16
1.3.2(b) Cathode Materials for LIB .....	16
1.3.2(c) Electrolyte for LIB.....	20
1.3.2(d) Separator Used in LIB .....	20
1.3.2(e) Current Research Goals in LIB .....	21
References.....	22
<b>2 Mg &amp; F doped LMR-NMC as an advanced cathode material for LIB.....</b>	<b>24</b>
2.1 Introduction.....	24
2.2 Structure of LMR-NMC.....	25
2.2.1 Why LMR-NMC.....	26
2.2.2 Mechanism for High-Voltage and Large Capacity .....	26
2.3 Challenges & Strategies .....	27
2.4 Experimentation.....	31
2.4.1 Material Preaprtion-Mg & F Doped LMR-NMC .....	31
2.4.2 Structural & Morphological Characterisation Techniques .....	32

2.4.3 Electrochemical Impedance Spectroscopy (EIS) Studies .....	35
2.4.4 Electrochemical Performance .....	36
2.5 Conclusion .....	39
References.....	40

## List of Figures:

1. Fig. 1.1 Ragone Plot for Various Rechargeable Battery Systems
2. Fig. 1.2 Schematic for Lithium-Ion Battery
3. Fig. 1.3 Current Status of Cathode and Anode Materials Used in LIB
4. Fig. 1.4 Structure of Layered, Spinel and Olivine Cathode Materials
5. Fig. 1.5 Electrolyte for Li-ion Batteries (a) The Family of Alkyl Carbonate Solvents (b) Schematic Presentation of Electrochemical Windows of Li Salt Solutions in Various Solvent Families
6. Fig. 2.1 (a) Crystal Structure of Layered Trigonal  $\text{LiMO}_2$  and (b) Crystal Structure of Layered Monoclinic  $\text{Li}_2\text{MnO}_3$ .
7. Fig. 2.2 Schematic Charge–Discharge Profiles of  $x\text{Li}_2\text{MnO}_3$  (1-x)  $\text{LiMO}_2$
8. Fig. 2.3 Schematic of Change in Crystal Structure of LMR-NMC During First Charge/Discharge Process
9. Fig. 2.4 (a) XRD of Mg-F Doped LMR-NMC (b) XRD of Mg-F Doped LMR-NMC  $\text{Li}_{1.2}\text{Ni}_{0.14}\text{Mn}_{0.55}\text{Co}_{0.102}\text{Mg}_{0.01}\text{O}_{2-x}\text{F}_x$
10. Fig. 2.5(a)(b) SEM Images of LMR-NMC, (c)(d) SEM Images of Mg-F Doped LMR-NMC
11. Fig. 2.6 EDX Characterizations of Mg-F Doped LMR-NMC Showing Ni, Mn, Mg, F, O and Co.
12. Fig. 2.7 Impedance Spectra of 10<sup>th</sup> cycle, Represented as Nyquist plots, of LMR-NMC & Mg-F Doped LMR-NMC
13. Fig. 2.8(a) Discharge Profile of LMR-NMC (b) Discharge Profile of Mg-F Doped LMR-NMC (c) Discharge Profile of Both LMR-NMC and Mg-F LMR-NMC for 30<sup>th</sup> Cycle
14. Fig. 2.9 (a) Cycle Life Data of Mg-F Doped LMR-NMC (b) Cycle Life Data of LMR-NMC
15. Fig. 2.10 dQ/dV Curves of Discharge Process for 10<sup>th</sup>, 20<sup>th</sup> & 30<sup>th</sup> Cycle of (a) LMR-NMC (b) Mg-F Doped LMR-NMC

## List of Tables:

1. Table.1 : Comparison of Energy Density of Various Cathode Materials
2. Table.2 : Rietveld Refinement of LMR-NMC and Mg-F Doped LMR-NMC



## Abstract

Lithium rich layered oxide (LMR-NMC) having composition  $\text{Li}_{1.2}\text{Mn}_{0.55}\text{Ni}_{0.15}\text{Co}_{0.10}\text{O}_2$  is considered as a potential candidate for cathode materials for high energy density lithium ion batteries for electric vehicles. The LMR NMC cathodes deliver capacity of  $> 250$  mAh/g when they are operated between 2.5 V and 4.8V. However, LMR-NMC suffer from some drawbacks which limits its application in electric vehicles like poor conductivity, less interfacial stability, structural instability, which leads to poor cycle life. The major issue with LMR-NMC is the voltage decay. The reason for voltage fade is the structure transformation from layered to spinel structure which reduces the operating voltage from 4V to 3V consequently reducing the energy density from 1000 Wh/kg to 750 Wh/kg.

Conductivity can be improved by using various conductive additive coatings. Interface can be stabilized by coating with metal oxides, metal phosphates. But the elimination of the detrimental spinel growth is a challenging task. The energy loss due to structural transformation from layered to spinel, leads to voltage decay has not been addressed properly till now.

Here we are presenting a method which improves interfacial stability also minimize the structural transformation, thus voltage decay can be minimized. It is found that Ni disordering is the major cause of structural transformation from layered to spinel. During cycling Ni disordering largely affects the electrochemical performance. So we have replaced a little amount of Ni in LMR-NMC with Mg. Also it is reported that replacing fluorine with oxygen also shows good electrochemical performance and cycling stability.

Both cation ( $\text{Mg}^{2+}$ ) and anion ( $\text{F}^-$ ) are doped synergically to LMR NMC. Mg doped LMR-NMC was synthesized by combustion process followed by LiF coating/ doping with LMR NMC by solid state synthesis. Structural and physical properties of doped and pristine LMR-NMC have been studied by XRD, SEM, EDX and (Rietveld refinements).

The electrochemical performance have been studied by galvanostatic charge-discharge cycling and electrochemical impedance studies. The role of Mg doping in LMR-NMC is to stabilize the crystal structure during cycling. Doping of Mg can help to mitigate the formation of spinel phase, as the introduction of  $\text{Mg}^{2+}$  could suppress the migration of transition metal ions into lithium sites thus help in stabilizing the structure. Adding Fluorine in crystal structure results in change in oxidation state of transition metal ions, also strong

M-F bond results in stabilizing the structure and decrease in oxygen release therefore enhance the cycling stability.

The Mg and F doped LMR NMC samples shows stable reversible capacities >300 mAh/g and sustain capacity retention >260 mAh/g at 1C rate, good cycle life and minimized voltage decay compared to pristine LMR-NMC.

# Chapter 1: Introduction to Lithium-Ion Battery

## 1.1 Motivation

Due to prolonged use of non-renewable energy sources, energy shortage is one of escalating problem in 21<sup>st</sup> century. The main source of energy for transportation in 21<sup>st</sup> century is the combustion of hydrocarbons. But due to use of these non-renewable fossil fuels leads to environmental pollution, CO<sub>2</sub> emission and global warming, and also the limited oil supply, force us to move on from these traditional energy sources to green sources like solar, hydroelectric, thermal and wind energy. The problem with these sources is that they suffer from uncontrollable and intermittent nature. So to maintain supply with demand, creating electrical-energy storage system is a crucial need. Rechargeable batteries are attractive options for such electrical energy storage system. There are many type of rechargeable batteries available in market like Ni-Cd, Lead-Acid, Li ion, Li-S. In comparison to other battery systems, lithium ion battery provides high energy density and power as shown in **Fig.1.1**.

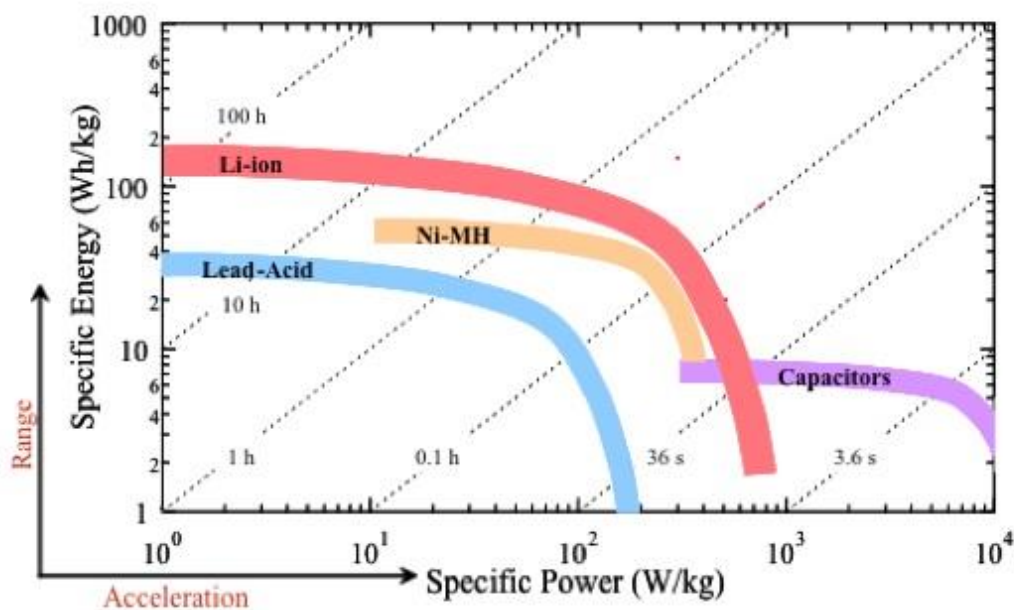


**Fig.1.1-** Ragone Plot for Various Rechargeable Battery Systems.

## 1.2 Why LIB among batteries

Li is the lightest metal, having weight about 6.94 g/mole. Also, the electrochemical equivalent weight of Li is equivalent to its atomic weight (6.94 g/mole) provides specific capacity of 3861mAh/g. Beside, Lithium has greatest electrochemical potential is 3.06 V. Because of high voltage, low molecular weight and high specific capacity of lithium, it provide high energy density lithium-ion battery.

Advantages of lithium-ion battery over other battery systems include:

1. Lithium has greater electrochemical potential (3.06 V)
2. Lighter than other
3. Low self-discharge (5-10 % per month)
4. No memory effect
5. Broad temperature range of operation (-40°C to +50°C)
6. High energy density (120-160 Wh/kg)
7. High life (>1000 cycles)

During last two and half decades, Li-Ion battery development has grown significantly and becoming first preference for portable devices, mobile phones, laptops, cameras and other electronic devices. Lithium-Ion Battery system is acknowledged as abutting solution for Electric and Hybrid electric vehicles due to its high energy density, high voltage (up to 5V), a longer and stable cycle life and simple reaction mechanism.

## 1.3 Introduction

As like other battery system lithium ion battery also consists of an anode, cathode and electrolyte which are separated by porous membrane (known as separator ex- polypropylene). Lithium ion intercalation chemistry was first demonstrated by Whittingham<sup>1</sup> in  $\text{TiS}_2$ . The layered transition metal dichalcogenides are able to intercalate a range of electron donating molecules and ions, in the van der Waals layers of structure. Whittingham used  $\text{TiS}_2$  as cathode and lithium as anode and  $\text{LiPF}_6$  as electrolyte dissolved in propylene carbonate for his electrochemical cell. During cycling single phase behavior enables to fully remove and reinsert lithium ions reversibly<sup>2,3</sup>. During cycling, the dendritic growth of lithium metal can cause short circuiting in the cell, which leads to explosion<sup>5</sup>.

In 1980 Goodenough<sup>6</sup> proposed Li ions are mobile in cubic close pack oxygen array of  $\text{LiMO}_2$  transition metal oxide which crystallizes in layered structure. On this basis, he discovered  $\text{LiCoO}_2$ , which appear as most promising cathode material for battery system.

$\text{LiCoO}_2$  was the first layered oxide to be commercialized as a cathode. Due to its high operating voltage of 3.7 V and high energy density is still commonly used in Li-ion batteries. For an insertion electrode for a Li-ion cell should have following properties: (a) operating voltage - high and stable, (b) host structure to de/insert a significant amount of Li ions to provide a high specific charge, (c) chemically and structurally stable in the operating voltage window, (d) good electronic and ionic conductivity, and (e) non-toxic.

In 1980 Yazami was the first to discover graphite as intercalation material. The reversible intercalation of lithium into graphite takes place in an electrochemical cell using a polymer electrolyte. Ultimately, this discovery by Yazami lead to the lithium graphite anode which are commonly used in commercial lithium ion batteries. Yazami also worked on other forms of graphite materials for application in lithium batteries, including graphite oxide and graphite fluoride.

In 1990, Li-Ion battery was first commercialized by Sony by using  $\text{LiCoO}_2$  as cathode and refinery coke as anode. It showed high capacity and good charge/discharge performance.

The biggest achievement of this system was the use of carbon material as anode (rather than Li metal as anode, formation of dendrites occur at high current densities<sup>6</sup>), provides sites for intercalation and deintercalation for Li ions reversibly. Even today we use the same chemistries for wide variety of applications.

The advantage of carbon-based anodes are long cycle life, low cost and abundance, also the graphite anode has significant drawbacks with regards to low gravimetric and volumetric specific capacity (372 mAh/g and 833 mAh/cm<sup>3</sup>). To replace current carbon-based anodes, Lithium–metal alloys such as lithium–tin are among the most promising materials because of their high capacity. In SONY's Nexelion battery, the use of these anodes includes nanostructured SnCo, which has increase in volumetric capacity (~50%) over the conventional battery<sup>7</sup>.

In December 2006, A123 systems of USA has come up with a new chemistry such as lithium ion (lithium iron phosphate) batteries for transportation and other commercial application based on power, abuse tolerance, durability and cost.

In 2009 A123's products are built using Nanophosphate chemistry, which delivers high power and energy density, extended cycle life and better safety performance.

### 1.3.1 Working Principle of Lithium-Ion Battery

Both cathode and anode used in LIBs are based on intercalation materials. In general lithium transition metal oxides or phosphates are used as cathodes and graphite is used as anode. It is the Li ion that are drifting repeatedly between the cathode and anode during charge and discharge (Fig.1.2). For intercalation of lithium ions both cathode and anode have unchangeable host with definite sites for lithium ions. The fully-charged negative plate is made of lithiated carbon, which is about 15 % lithium by weight and has about the same electrochemical potential as metallic lithium.

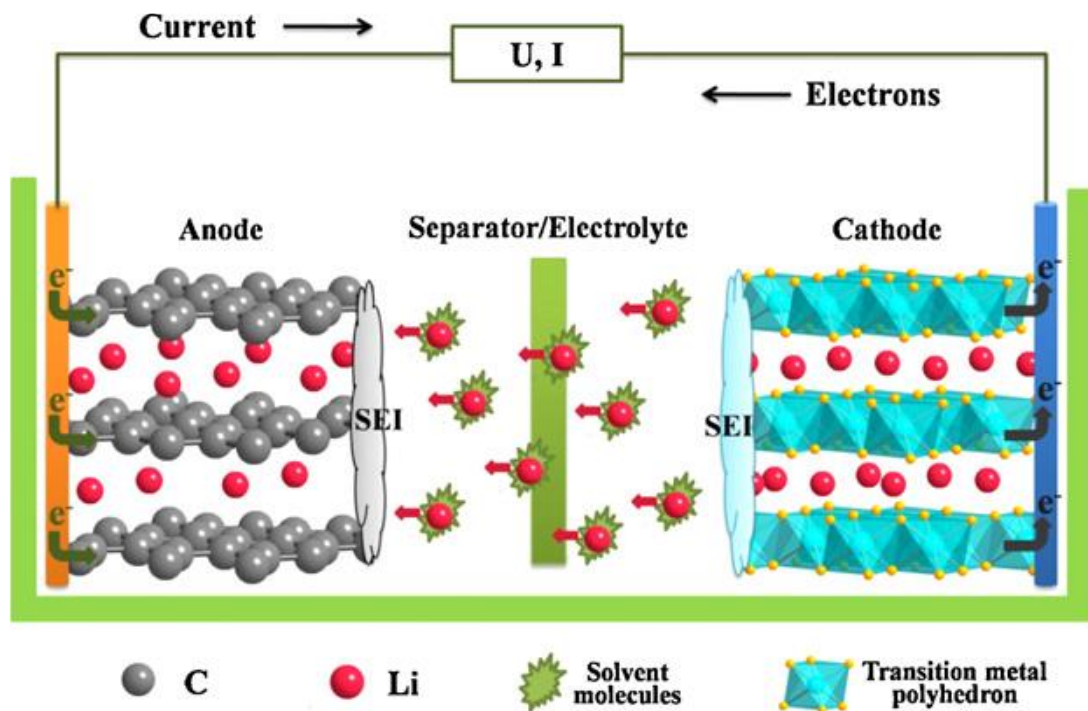
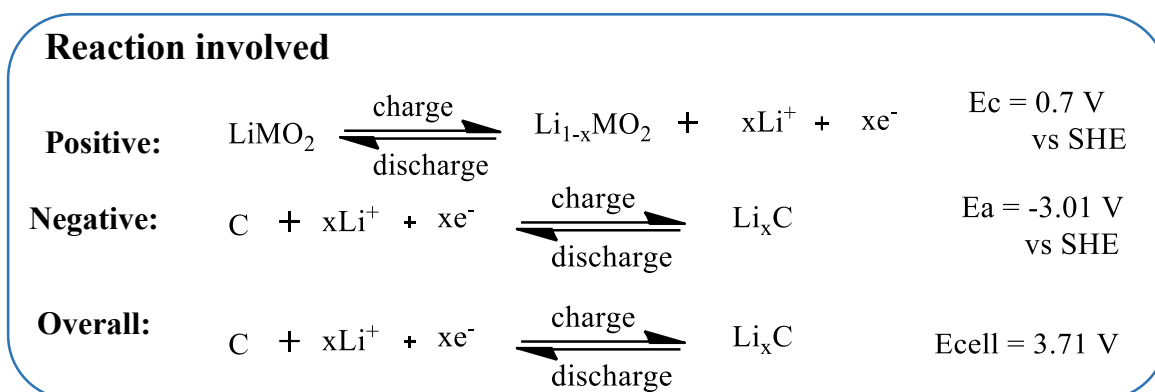


Fig.1.2: Schematic for Lithium-Ion Battery

Following redox equations describes the charging process of lithium-ion battery system.



In lithium-ion battery system, intercalation/de-intercalation reaction play an important role, without changing the basic crystal structure lithium ion get inserted/de-inserted into interstitial sites.

Initially, all of the lithium ions occupy space in cathode sites and the system is said to be in discharge state. During charging, Lithium ions are extracted from cathode host and move through the non-aqueous electrolyte namely lithium based salts are dissolved in alkyl carbonate solvents, and intercalate into anode host. During charging lithium ion move from cathode to anode and electrons move in external circuit. During discharging, whole process get reversed. In Lithium ion battery system, electric energy is stored in the form of electrochemical energy.

A polymer based separator (micro-porous membrane) is used between cathode and anode to prevent shorting between the electrodes and it allows the passage of ions and electrolyte.

The electrolyte should be electronically insulating and ionically conducting to ions.

During the 1<sup>st</sup> cycle at extreme cycling conditions (<1.2V for anodes and >4.2 V for cathode) a thin layer of salt decomposition products are formed on surface of electrodes called SEI layer (Solid-electrolyte-interphase).

There is a large capacity difference between lithium metal and other anode material. But Lithium, metal has safety concern caused by dendrite growth of lithium during electrochemical cycling. On the other hand, capacities of anode materials (300-500 mAh/g) is much greater than that of cathode (120-180 mAh/g). The capacity, cycle life, thermal stability are not very high for many applications like grid storage and electric vehicles. So research and development (R&D) is fairly under progress for both cathode and anode.

### 1.3.2 Current status of Lithium-Ion Battery

#### a. Anode material for lithium ion battery

Graphite was introduced in LIBs by Sony as an anode material. Even today graphite is used as anodes in battery system.

Beside graphite, Tin (Sn) (1000 mAh/g) and Silicon (Si) (4200 mAh/g) based materials have been developed over the years which can be used as anode materials for LIBs. The main drawback of these materials is that during lithiation large volume change takes place so huge amount of mechanical stress develop and also pulverization of electrode material take place during charge/discharge cycles. The research in these aspects are under progress.

Other than graphite, Sn and Si based compounds, transition metal oxide MO (M= Co,Ni,Cu,Fe) based conversion anodes can be used in LIB. These transition metal oxide anodes shows theoretical capacity of ~500-1000 mAh/g.

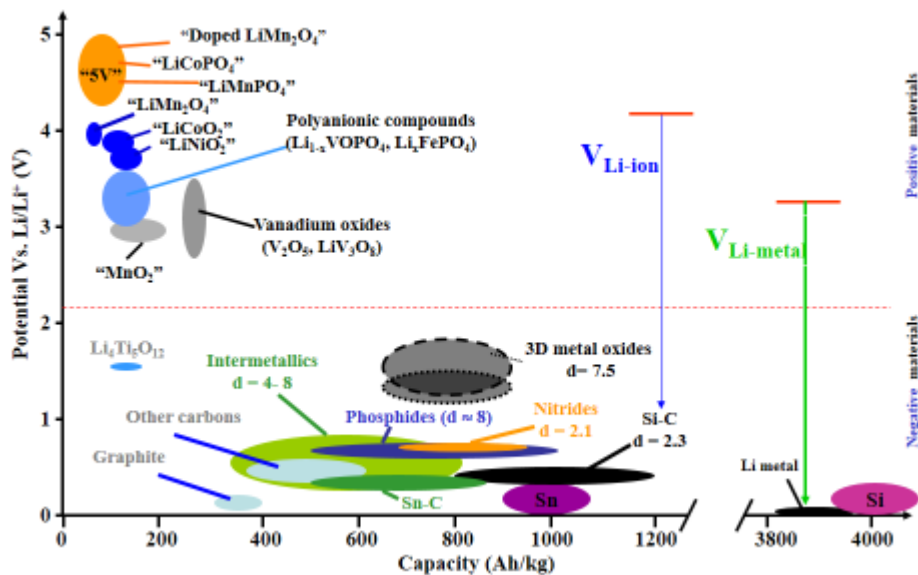


**Fig1.3.** Current Status of Cathode and Anode Materials Used in LIB.



## b. Cathode material for lithium ion battery

In 1990, when for the first time  $\text{LiCoO}_2$  came to the market as a cathode material for rechargeable lithium ion battery, the focus of research moved to intercalation material of transition metal oxide as cathode for lithium ion battery system.

Mainly cathodes categories in following three categories:

1. Layered oxides  $\text{LiMO}_2$
2. Spinel compounds  $\text{LiM}_2\text{O}_4$
3. Olivine based compounds  $\text{LiMPO}_4$

Nearly all researches are focused on these materials and their derivatives. In recent years Silicates, borates are also gaining attention.

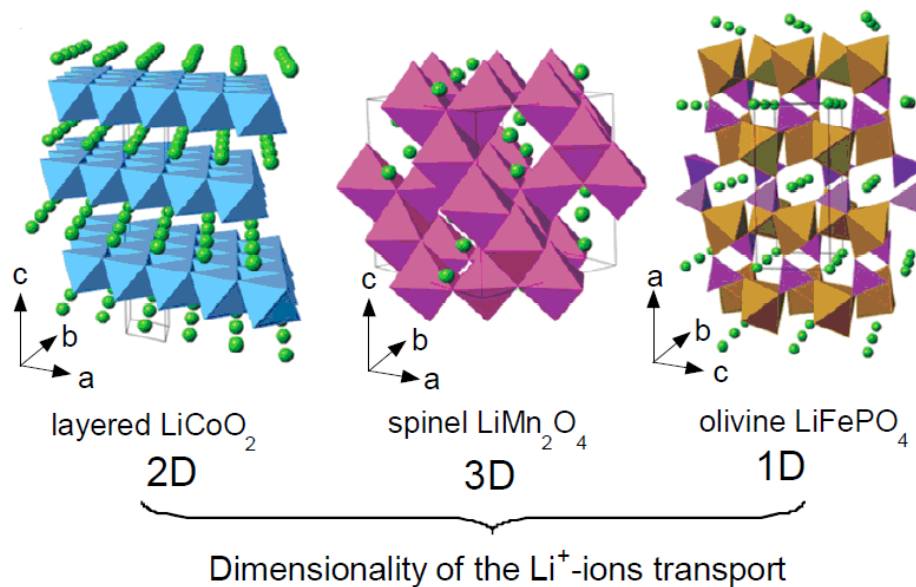


**Fig1.4.** Structure of Layered, Spinel and Olivine Cathode Materials

### i) Layered oxide $\text{LiMO}_2$

The commercial  $\text{LiCoO}_2$  delivers specific capacity  $140\text{mAh/g}$  (half of its theoretical capacity). This is mainly due to structure instability and also Co is toxic and expensive. The poor electrochemical properties of  $\text{LiCoO}_2$  are mainly due to the dissolution of Co ions into electrolyte at high voltage<sup>8</sup>. Various metal oxides were coated onto  $\text{LiCoO}_2$  to solve this problem<sup>9-12</sup>. The metal oxide coating or substitution effectively reduce Co dissolution, so at the high-voltage region capacity retention increases<sup>13,14</sup>. The  $\text{LiCoO}_2$  derivative where Co is

partially or fully substituted by other metal ions like Ni and Mn. Certain other materials were synthesized like  $\text{LiNi}_{0.5}\text{Mn}_{0.5}\text{O}_2$  and  $\text{LiCo}_{1/3}\text{Ni}_{1/3}\text{Mn}_{1/3}\text{O}_2$  (NMC) with different ratios of metal ions and electrochemical characterization was done. It is reported that in  $\text{LiNi}_{0.5}\text{Mn}_{0.5}\text{O}_2$ , the Li diffusion coefficient is lower than that in  $\text{LiCoO}_2$  by one magnitude of order<sup>1</sup>.

Li-Co-Ni-Mn-O also called NMC is one of the derivatives of  $\text{LiCoO}_2$ . NMC<sup>15</sup> ( $\text{LiCo}_{1/3}\text{Ni}_{1/3}\text{Mn}_{1/3}\text{O}_2$  first introduced by Ohzuku's group having hexagonal structure) have following advantages:

- a. Moderate thermal stability
- b. High rechargeable capacity (more than 150 mAh/g) at high rates,
- c. Better cycling stability
- d. Low cost
- e. Less Toxic

NMC is considered as potential cathode material for coming generation.

In NMC, it is considered that during charging oxidation of transition metal ions occur like this  $\text{Ni}^{2+}$  to  $\text{Ni}^{3+}$ ,  $\text{Ni}^{3+}$  to  $\text{Ni}^{4+}$ ,  $\text{Co}^{3+}$  to  $\text{Co}^{4+}$ .  $\text{Mn}^{4+}$  ion behave as spectator and maintain the structure stability<sup>16,17</sup>.

Layered NMC also exhibits some problems like rapid capacity fading, voltage fading, inferior rate capability which limits its use in vehicle application.

Several further modification were done in order to improve the electro-chemical performance of NMC such as by decrement of Co, also gives the same effect. The one tremendous thing discovered was the addition of extra lithium ions, which helps to improve the material capacity.  $\text{Li}[\text{Li}_x\text{Ni}_{(1-2x/3)}\text{Mn}_{(2-x/3)}]\text{O}_2$  was the first lithium rich layered oxide discovered by Dahn group in 2001, is considered as solid solution of two layered materials  $\text{LiMO}_2$  (M=Ni, Mn and/or Co) and  $\text{Li}[\text{Li}_{1/3}\text{Mn}_{2/3}\text{O}_2]$  (can be represented as  $\text{Li}_2\text{MnO}_3$ ), delivers more than 230mAh/g capacity which is much more than conventional  $\text{LiCoO}_2$ ,  $\text{LiNi}_{1/3}\text{Mn}_{1/3}\text{Co}_{1/3}\text{O}_2$ ,  $\text{LiMn}_2\text{O}_4$ , and  $\text{LiFePO}_4$ . But due to some flaws like capacity fading at high voltage and poor rate capability, again further alterations were done, Co was added in order to improve crystal structure and it was observed that it also helps in upgrading the electrochemical performance.

## ii) Olivine compounds $\text{LiMPO}_4$

In 1997, after the study of electrochemical properties of olivine phase, research interest for cathodes move on olivines ( $\text{LiFePO}_4$ ), also it is of low cost and environmentally safe. The material is gaining so much focus due to its structure stability (because of polyanion)<sup>18,19</sup> and also can minimize oxygen loss happening in layered and spinel compounds. The  $\text{LiFeO}_4$  delivers capacity of 130mAh/g and its theoretical capacity is 170mAh/g. the main disadvantage for this is disadvantage occur at 3.5V, which is less than that of  $\text{LiCoO}_2$ . Other than  $\text{LiFeO}_4$ , other olivine compounds are also available on basis of different redox couple, the voltage is 4.1 V for  $\text{LiMnPO}_4$ <sup>18</sup> 4.8 V for  $\text{LiCoPO}_4$ <sup>20</sup> and 5.1 V for  $\text{LiNiPO}_4$ . The main challenge for  $\text{LiFePO}_4$  is poor rate capability caused by low electronic conductivity and comparable low Li-ion diffusion<sup>21</sup>.  $\text{LiMnPO}_4$  provides higher theoretical energy density ( $701 \text{ Wh/kg} = 171 \text{ mAh/g} \times 4.1 \text{ V}$ ) due to high potential than that of  $\text{LiFePO}_4$  ( $586 \text{ Wh/kg} = 170 \text{ mAh/g} \times 3.45 \text{ V}$ ). On basis of these theoretical calculations, research focus moved on to  $\text{LiMnPO}_4$ . But  $\text{LiMnPO}_4$  faces a lot of problems, such as passivation phenomenon upon delithiation, Jahn-Teller distortion due to  $\text{Mn}^{3+}$ , due to the large volume change interface strain occur between  $\text{LiMnPO}_4$  and  $\text{MnPO}_4$ , and the metastable nature of the delithiated  $\text{MnPO}_4$  phase. So taking all this in consideration Mn was substituted in  $\text{LiFePO}_4$  to achieve good electrochemical performance. The larger ionic radius of  $\text{Mn}^{2+}$ , provides a wider channel for Li diffusion which enhances the mobility of the Li ion. 10% substitution ( $\text{M} = \text{Fe}_{0.9}\text{Mn}_{0.1}$ ) was chosen<sup>22</sup>, and it showed better results. The reason to choose only 10% because if the amount of Mn is much smaller then only small change is observed otherwise the two-step voltage plateau observed if the Mn composition is larger which might cause problems in battery applications.

## iii) Spinel compounds $\text{LiM}_2\text{O}_4$

In 1983, Thackeray proposed spinel  $\text{LiMn}_2\text{O}_4$  as the cathode of the lithium ion battery<sup>23,24</sup>. The structure of  $\text{LiM}_2\text{O}_4$  is based on three dimensional host. The diffusion of lithium ions also three dimensional due to vacancies in transitional metal layer.  $\text{LiMn}_2\text{O}_4$  was the first spinel compound with capacity 148mAh/g.  $\text{LiMn}_2\text{O}_4$  faces a lot of problem like capacity fading. The reason behind this was mainly the dissolution of  $\text{Mn}^{2+}$  in electrolyte, generation of new phases during cycling<sup>25,26,27</sup>. Certain modification were done in  $\text{LiMn}_2\text{O}_4$  based on substitution of Mn by other metal ions and it was found that  $\text{LiNi}_{0.5}\text{Mn}_{1.5}\text{O}_4$  show best results.  $\text{LiNi}_{0.5}\text{Mn}_{1.5}\text{O}_4$

(NMS), as compare to  $\text{LiMn}_2\text{O}_4$  spinel, oxidation/reduction reactions are switched from  $\text{Mn}^{3+}/\text{Mn}^{4+}$  to  $\text{Ni}^{2+}/\text{Ni}^{4+}$  and voltage is also lifted from 4.1 V to 4.7 V. Due to partial substitution of Mn ion by Ni in NMS the problem of dissolution of  $\text{Mn}^{2+}$  ions in electrolyte also resolved<sup>28</sup>. The reason why NMS is an interesting material is its increase in energy density (High plateau voltage at 4.7 V) of more than 30% than the conventional lithium manganese spinel).

### c. Electrolyte

While choosing a compound as an electrolyte following points should be considered:

- High  $\text{Li}^+$  ion conductivity
- Wide electrochemical window
- Retention of electrode/electrolyte interface
- Chemical stability
- Safety (non-flammable)

Hence by considering all these characteristics, alkyl carbonates were found as a best and most suitable solvent for electrolyte in lithium-ion battery system. In alkyl carbonates, ethylene carbonate (EC) or diethyl or dimethyl carbonate (DEC or DMC) or ethyl methyl carbonate (EMC) can be used as an electrolyte. The commonly used electrolyte is a mixture of EC, DMC containing complexes of lithium ions. The non-coordinating anion salts are generally used in non-aqueous electrolytes such as **lithium hexafluorophosphate ( $\text{LiPF}_6$ ) (Best salt)**, lithium hexafluoroarsenatemonohydrate ( $\text{LiAsF}_6$ ), lithium perchlorate ( $\text{LiClO}_4$ ), lithium tetrafluoroborate ( $\text{LiBF}_4$ ) and lithium triflate ( $\text{LiCF}_3\text{SO}_3$ ).

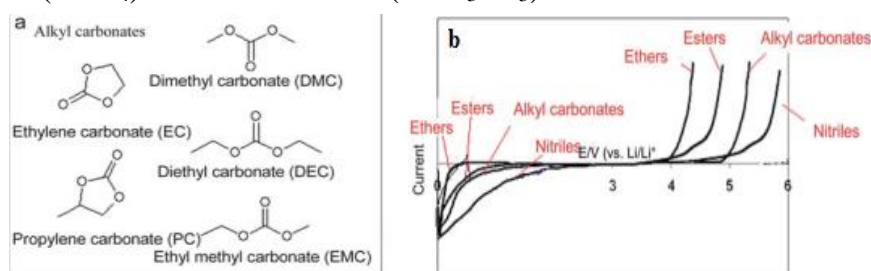


**Fig. 1.5:** Electrolyte for Li-Ion Batteries. (a) The family of Alkyl Carbonate Solvents. (b) Schematic Presentation of Electrochemical Windows of Li Salt Solutions in Various Solvent Families

#### **d. Separator**

Both cathode and anode are separated with each other by a Separator, a micro-porous membrane which mainly prevent the shorting of two electrodes.

**Polypropylene / Polyethylene (PP/PE/PP)** used as a separator in lithium ion battery.

#### **e. Current research goals for lithium-ion batteries**

State-of-the-art lithium-ion batteries use layered transition metal (TM) oxides,  $\text{LiMO}_2$ , where M can be any combination of Mn, Ni, Co or Mn based spinels or  $\text{LiFePO}_4$  as cathodes and graphitic carbon as anode<sup>5,33,34</sup>. The nominal capacity of most of these cathodes when cycled up to 4.2 V range in between 140-180  $\text{mAhg}^{-1}$ . This is only half the specific capacity of graphite anode (372  $\text{mAhg}^{-1}$ ). Thus, there has been an intense research activity during the last decade to develop high capacity or high energy cathodes for lithium-ion batteries. Lithium and manganese rich TM oxide composite cathodes given by the generic formula,  $x\text{Li}_2\text{MnO}_3 \cdot (1-x)\text{LiMO}_2$  that has approximately double capacity of layered TM oxides (about 280  $\text{mAhg}^{-1}$ ) but needs to be electrochemically cycled to a voltage  $> 4.5 \text{ V}$ <sup>35,36</sup>.

## References:

1. M.S. Whittingham, *Science* 1976, **192**, 1126.
2. M. S. Whittingham, *Chem. Commun.* 1974, **9**, 328.
3. G. V. Subba Rao and J. C. Tsang, *Mater. Res. Bull.* 1974, **9**, 921.
4. M.S. Whittingham, *J. Electrochem. Soc.* 1976, **123**, 315.
5. M.S. Whittingham, *Chem. Rev.* 2004, **104**, 4271.
6. K. Mizushima, P.C.Jones, J.B. Goodenough, *Mater. Res. Bull.* 1980, **15**, 783.
7. M.S. Whittingham, *MRS Bull.* 2008, **33**, 411.
8. G. G. Amatucci, J. M. Tarascon, *Solid State Ionics*, 1996, **83**, 16.
9. M. Mladenov, R. S. Stoyanova, E. Zhecheva, and S. Vassilev, *Electrochem. Commun.* 2001, **3**, 410.
10. H. Wang, Y.I. Jang, B. Huang, D.R. Sadoway, Y.M. Chiang, *J. PowerSources*, 1999, **594**, 81.
11. J. Cho, Y. J. Kim, and B. Park, *Chem. Mater.*, 2000, **12**, 3788.
12. M. C. Fredel and A. R. Boccaccini, *J. Mater. Sci.*, 1996, **31**, 4375.
13. A. M. Kannan, L. Rabenberg, and A. Manthiram, *Electrochem. Solid-State Lett.* 2003, **6**, A16.
14. Z. Chen and J. R. Dahn, *Electrochem. Solid-State Lett.* 2002, **5**, A213.
15. T. Ohzuku, Y. Makimura, *Chem. Lett.*, 2001, 642.
16. N. Yabuuchi, T. Ohzuku, *J. Power Sources*, 2005, **146**, 636.
17. K.M. Shaju, P.G. Bruce, *Adv. Mater.*, 2006, **18**, 2330.
18. A.K. Padhi, *J. Electrochem. Soc.* 1997, **144**, 1188.
19. A.K. Padhi, K.S. Nanjundaswamy, C. Masquelier, S. Okada, J.B. Goodenough, *J. Electrochem. Soc.* 1997, **144**, 1609.
20. J. Wolfenstine, J. Allen, *Journal of Power Sources* 2004, **136**, 150.
21. S.Y. Chung, J.T. Bloking, Y.M. Chiang, *Nat. Mater.* 2002, **1**, 123.
22. Kyung Tae Lee, Kyung Sub Lee, *J. Power Sources*, 2009, **189**, 435.
23. M.M. Thackeray, W.I.F. David, P.G. Bruce, J.B. Goodenough, *Mater. Res. Bull.* 1983, **18**, 461.
24. J.B. Goodenough, M.M. Thackeray, W.I.F. David, P.G. Bruce, *Revue de Chimie Minerale* 1984, **21**, 435.
25. D. Aurbach, M.D. Levi, K. Gamulski, B. Markovsky, G. Salitra, E. Levi, U. Heider, L.Heider, R. Oesten, *J. Power Sources* 1999, **81**, 472.
26. Y.Y. Xia, Y.H. Zhou, M. Yoshio, *J. Electrochem. Soc.*, 1997, **144**, 2593.

27. Y.J. Shin, A. Manthiram, *J. Electrochem. Soc.* 2004, **151**, 204.
28. *Electrochem. Comm.* 2013, **34**, 48.
29. Jiajun Chen, *Materials*, 2013, **6**, 156.
30. Bo Xu, Danna Qian, Ziyang Wang, Ying Shirley Meng, *Mater. Sci. Eng., R*, 2012, **73**, 51.
31. J.-M. Tarascon & M. Armand, *Nature*, 2001, **414**.
32. J.-M. Tarascon, *Phil. Trans. R. Soc. A*, 2010, **368**, 3227.
33. V. Etacheri, R. Marom, R. Elazari, G. Salitra and D. Aurbach, *Energy Environ. Sci.*, 2011, **4**, 3243.
34. M. M. Thackeray, C. Wolverton and E. D. Isaacs, *Energy Environ. Sci.*, 2012, **5**, 7854.
35. Y. Kim, G. M. Veith, J. Nanda, R. R. Unocic, M. Chi and N. J. Dudney, *Electrochim. Acta*, 2011, **56**, 6573.
36. M. M. Thackeray, S.-H. Kang, C. S. Johnson, J. T. Vaughey, R. Benedek and S. A. Hackney, *J. Mater. Chem.*, 2007, **17**, 3112.

## Chapter 2: Magnesium & Fluorine doped LMR-NMC as an advanced cathode material for lithium ion battery

### 2.1 Introduction

LMR-NMC (Lithium manganese rich, nickel manganese cobalt oxide  $\text{Li}_{1.2}\text{Mn}_{0.55}\text{Ni}_{0.10}\text{Co}_{0.102}\text{O}_2$ ) was derived from NMC ( $\text{LiMn}_{1/3}\text{Ni}_{1/3}\text{Co}_{1/3}\text{O}_2$ ). NMC having hexagonal structure was first introduced by Ohzuku's group. Due to combination of nickel, cobalt, manganese NMC provide various advantages over  $\text{LiCoO}_2$  like lower cost, less toxic, mild thermal stability, better cycling stability at high temperature and high reversible capacity. In NMC lithium extraction occur due to oxidation/reduction of  $\text{Ni}^{2+}/\text{Ni}^{4+}$ ,  $\text{Co}^{3+}/\text{Co}^{4+}$  and  $\text{Mn}^{4+}$  remain as inactive and helps in structure stability.

Layered NMC exhibits rapid capacity fading and inferior rate capability which limits its use in vehicle application. The problem with NMC is that cation mixing occur between lithium and nickel ions which deteriorates its electrochemical performance. This is because ionic radii of both  $\text{Li}^+$  (0.76Å) and  $\text{Ni}^{2+}$  (0.69Å) are very close so  $\text{Ni}^{2+}$  occupy the sites of  $\text{Li}^+$  and block the pathway of lithium diffusion. In order to minimize drawbacks of NMC, extra lithium was added to improve its performance.

It was found that increasing Co content could suppress cation mixing but at the same time decrease in capacity observed, while increasing Ni content could increase capacity but cation mixing increase due to this. So Ni, Mn, Co contents were optimized and the content of Co, Mn, and Ni in LMR-NMC found to be promising cathode material.

Thackeray and co-workers proposed that LMR-NMC is a two component composites between  $\text{Li}_2\text{MnO}_3$  and  $\text{LiMO}_2$ <sup>1</sup>. Thus for  $\text{Li}_{1.2}\text{Mn}_{0.55}\text{Ni}_{0.10}\text{Co}_{0.10}\text{O}_2$  two component notation can be written as  $0.5\text{Li}_2\text{MnO}_3 - 0.5\text{LiNi}_{0.375}\text{Co}_{0.25}\text{Mn}_{0.375}\text{O}_2$ . Lithium rich NMC can deliver capacity more than 250 mAh/g with an operating voltage higher than 4.5V.

$\text{Li}_2\text{MnO}_3$  phase in LMR-NMC is considered as best stabilized component as it is electrochemically inactive over a wide potential range (2.2-4.5V) but above 4.4V it is electrochemically active and can contribute towards irreversible capacity loss in first cycle<sup>2-5</sup>. Thus when cycled between 2.0-4.8V, LMR-NMC provides high reversible capacity (>300mAh/g) and high energy density (>1000Wh/kg)<sup>6,7</sup>.



## 2.2 Structure of LMR-NMC:

LMR-NMC also represented by the formula  $x\text{Li}_2\text{MnO}_3 (1-x)\text{-LiMO}_2$ . Both  $\text{Li}_2\text{MnO}_3$  and  $\text{LiMO}_2$  are isostructural both crystallize in layered rock-salt structure, due to this composite forms and in one layer  $\text{Li}^+$  ions are present and other layer contains mixture of  $\text{Li}^+$ ,  $\text{Mn}^{4+}$  and  $\text{M}^{3+}$  ions, both layers are alternatively packed in a cubic close array of oxygen<sup>8</sup>. In  $\text{Li}_2\text{MnO}_3$  layer, both  $\text{Li}^+$  and  $\text{Mn}^{4+}$  ions occupy transition metal layer, while for  $\text{LiMO}_2$  transition metal layer occupied by transition metal ions.

In transition metal layer both  $\text{Li}^+$  and  $\text{Mn}^{4+}$  due to this symmetry of  $\text{Li}_2\text{MnO}_3$  reduces.

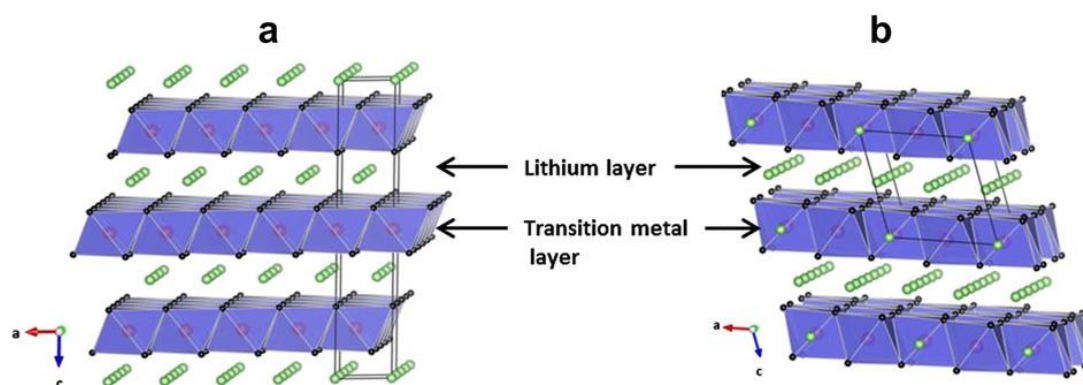


**Fig. 2.1:** (a) Crystal Structure of Layered Trigonal  $\text{LiMO}_2$  and (b) Crystal Structure of Layered Monoclinic  $\text{Li}_2\text{MnO}_3$ . In  $\text{Li}_2\text{MnO}_3$  Structure, Lithium ions occupy transition metal layer as well as lithium layer.

Thus, the structure of LMR-NMC can be derived from layered  $\text{LiMO}_2$ , with the excess lithium ions occupy transition metal layer, filling all the octahedral sites of cubic close pack arrays of oxygen. The long range/short-range cation ordering generates between transition metal ions due to the presence of extra lithium ions in transition metal layer in  $\text{Li}_2\text{MnO}_3$  phase<sup>9</sup>.

### 2.2.1 Why LMR-NMC?

Layered transition metal oxides  $\text{LiMO}_2$ , spinels  $\text{LiM}_2\text{O}_4$ , and olivine  $\text{LiMPO}_4$  ( $\text{M} = \text{Mn}, \text{Ni}, \text{Co}$  or  $\text{Mn}$ ) are used as cathodes and graphite as anode in lithium ion battery. When cycled up to 4.2V the nominal capacity observed for these cathode materials is in range of 140-180mAh/g<sup>10,11,12</sup>, which is half of the specific capacity of the graphite anode (372 mAh/g). But lithium-

rich TM oxide composite cathodes provide almost double capacity (280mAh/g) than layered TM oxide, when cycled above 4.5V.

Material Type	Nominal Voltage (V)	Capacity (C/5 rate) (Ah/Kg)	Maximum achievable energy density (Wh/Kg)
LiFePO <sub>4</sub>	3.3	170	560
LiCoO <sub>2</sub>	3.7	140	520
LiNi <sub>1/3</sub> Mn <sub>1/3</sub> Co <sub>1/3</sub> O <sub>2</sub> (NMC)	3.8	160	608
Li <sub>1+x</sub> (NiMnCo)O <sub>2</sub> (Li-Rich NMC)	3.8	280	1064

**Table 1:** Comparison of Energy Density of Various Cathode Materials

### 2.2.2 Mechanism for high-voltage and large capacity

The capacity of LMR-NMC family is >250mAh/g when cycled to the voltage of 4.8V. The mechanism for high capacity of LMR-NMC shows that<sup>13,14,15</sup> LMR NMC has two distinct region during first charge as shown in **Fig.2.2**<sup>16</sup>. During first charge, lithium ion are extracted from lithium layer, contribute to an increase in capacity up to cell voltage of 4.4V as clearly visible in region A. So initial sloping region A corresponds to oxidation of transition metal ions to M<sup>4+</sup>. The capacity measured in the potential range of 2.5–4.4V shows that only LiMO<sub>2</sub> is activated.

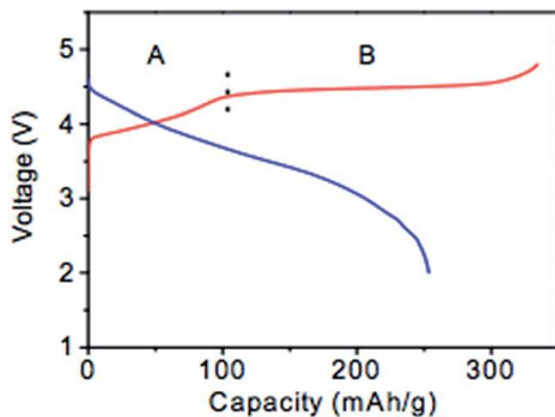


**Fig.2.2-** Schematic Charge–Discharge Profiles of  $x\text{Li}_2\text{MnO}_3 (1-x) \text{LiMO}_2$

Beyond 4.4V, a voltage plateau is observed in the range of 4.4-4.65V, with charge capacity of >260mAh/g. In the region B, capacity increase is due to extraction of lithium ions from  $\text{Li}_2\text{MnO}_3$  phase<sup>17,18</sup>. That means beyond 4.4V  $\text{Li}_2\text{MnO}_3$  component gets activated, by decomposition to  $\text{Li}_2\text{O}$  and  $\text{MnO}_2$ . Due to formation of  $\text{MnO}_2$  phase Li ions can reversibly intercalate in  $\text{MnO}_2$  sites.

During first charge, the main source of electrons and extraction of Lithium ions is oxidation of  $\text{O}^{2-}$  to  $\text{O}_2$ , which also make sure that  $\text{M}^{4+}$  can't be oxidized further which is coordinated to six oxide ions in an octahedral site<sup>19</sup>. This irreversible loss of oxygen during first charge provides reduction of  $\text{M}^{4+}$  to lower oxidation states. Thus, the first charge profile is different due to oxygen loss and activation of  $\text{Li}_2\text{MnO}_3$  phase.

### 2.3 Challenges and strategies:

LMR-NMC provides high capacity >250 mAh/g and voltage ~4V is considered to be an attractive candidate for LIB. Apart from of delivering high capacity at high operating voltage, LMR-NMC follows the drawbacks during repeated electrochemical cycles which limits its application in hybrid and Electrical vehicles:

- Inferior cycling stability
- Capacity fade
- Voltage fade
- Poor rate capability
- Oxygen loss

The reason for poor rate performance of LMR-NMC is associated with poor electron transfer because of insulating  $\text{Li}_2\text{MnO}_3$  component (having low electronic conductivity) and formation of thick SEI (solid-electrolyte-interface) layer formed during charge/discharge by the reaction of cathode surface and electrolyte at >4.4 V.

The capacity loss is mainly due to release of oxygen results in vacancies of oxide ion during first charge, which at high operating voltage (~4.8V) quickly react with carbonate based solvents and form inactive salt decomposition products on the surface. Also the other reason for capacity fade is difficulty for  $\text{Li}^+$  trapping in negative SEI film during 1<sup>st</sup> cycle.

The fast energy fading of LMR-NMC during cycling is also due to rise in impedance which may be due to occupancy of lithium atom in different oxide sites during charge/discharge. Cell resistance increases mainly due to degradation of electrode and electrolyte constituents at high

operating voltage and also may be due to growing surface films which slow down the charge carrier transport.

It is also considered that low columbic efficiency of material is due to removal of oxygen vacancies during first charge which is due to irreversible removal of  $\text{Li}_2\text{O}$  from crystal structure. The  $\text{Li}_2\text{O}$  removal from lattice causes rearrangement of transition metal ions which leads to structural instability, causing capacity fade during cycling<sup>20</sup>.

The voltage fade occur due to the transformation of structure from layered to spinel (**Fig.2.3**). This is mainly due to the deep lithiation - delithiation, during cycling. The main reason for structure transformation from layer to spinel is migration of transition metal from octahedral sites (M layer) to tetrahedral sites (Li layer) without changing oxygen host<sup>21</sup>. A theoretical simulation predicts that transformation of layered to spinel occur via formation of dumbbell structure. Formation of Dumbbell structure facilitates the migration of transition metal ion to lithium layer to form a spinel phase<sup>22</sup>.

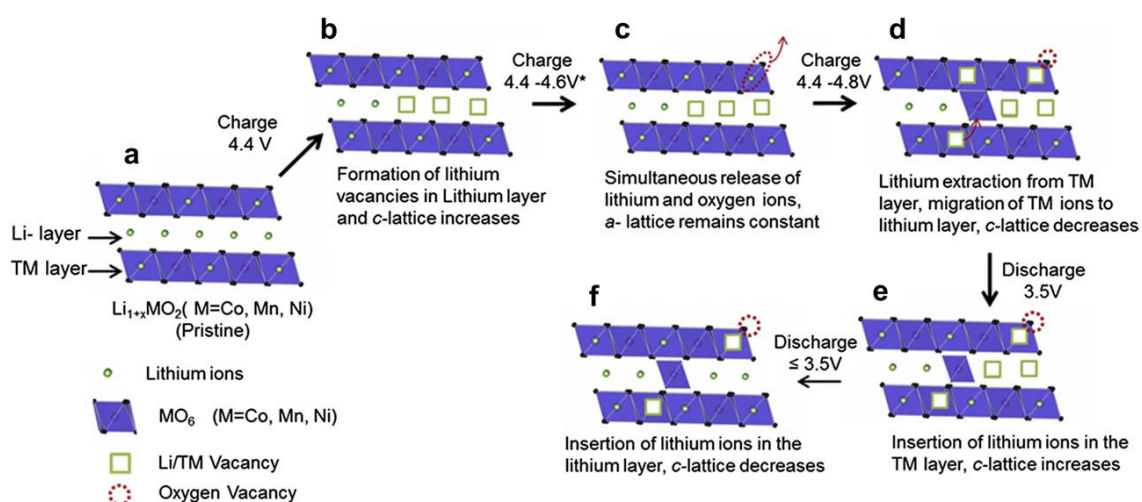


**Fig. 2.3-** Schematic of Change in Crystal Structure of LMR-NMC during First Charge/Discharge Process

The reason of poor cyclability is due to low electronic and ionic conductivity of LMR-NMC and interfacial instability.

Both voltage fade and capacity fade are accompanied with internal phase transition. On basis of some results it is observed that voltage fade is unaffected by coatings, cation doping and substitution, whereas, the cut-off voltage and cation ordering in crystal structure influence voltage fade. Voltage fade get lowers by lowering the cut-off voltage. No voltage fade observe

when 4.3V is used as upper cut-off voltage as cycling voltage. Also, by improving Li mobility and cation disorder, voltage fade can be mitigated.

Thus to improve electrochemical performance several processes have been done:

#### 1. Surface modification to improve capacity fading:

- (i) Surface modification by thin layer of metal compounds like halides  $\text{AlF}_3$ , oxides  $\text{ZnO}$ ,  $\text{ZrO}_2$ ,  $\text{Al}_2\text{O}_3$ , phosphates  $\text{FePO}_4$ ,<sup>22,23,24</sup> helps in protecting interface of cathode material from attack of acidic species like HF and oxidation of solvents( carbonate based solvents) at high voltage<sup>25,26</sup>. Thus capacity fading can be altered by surface modification.
- (ii) Surface modification does not help structure transformation thus voltage fade is not mitigated.

#### 2. Improve electrochemical performance through elemental doping:

Elemental doping is another effective way to help in enhancing electrochemical performance. By previous studies it is indicated that cation disorder occur during  $\text{LiMO}_2$  preparation because ionic radii of both  $\text{Li}^+$  (0.76Å) and  $\text{Ni}^{2+}$  (0.69Å) are similar. Thus during cycling  $\text{Ni}^{2+}$  can occupy  $\text{Li}^+$  sites in lithium layer after calcination<sup>27,28</sup>. So this phenomenon gives an idea to achieve lithium sites by cation doping in lithium rich layered oxide cathode materials. For this, cation should have ionic radii close to  $\text{Li}^+$  to occupy preferential sites, should be electrochemically inert to prevent structure variation. Cation doping has already done before with several cations such as Co, Al, Fe, Cr, Mg, Ru to improve electrochemical performance<sup>29-35</sup>.

It is reported that sodium (Na) doping inhibit the spinel growth. Introduction of Na ion in crystal expand lithium slab space, thus facilitates the lithium ion diffusion. Also Na doping helps in improving reversible capacity (307mAh/g) and rate capability (139mAh/g at 8C)<sup>36,40,41</sup>.

It has been reported that doping of manganese content with 0.02 Aluminum improves the rate capability of lithium rich layered oxide by increasing diffusion of lithium intercalation/deintercalation, as doping of aluminum increases c lattice parameter<sup>37</sup>.

It is reported that doping of potassium (K) on the Li layer suppresses the layered to spinel phase transition, but this effect is attributed to the suppressed formation of tri-vacancies in the Li layer and aggravated steric hindrance for spinel growth with the large  $K^+$  ions<sup>39</sup>. Doping of anion is helpful in improving electrochemical performance. This is because the fluorine doped compounds ( $Li_{1+x}M_yO_{2-z}F_z$ ) have smaller lattice parameter than lithium rich layered oxides ( $Li_{1+x}M_yO_2$ ) because of change in oxidation state of transition metal ions due to fluorine substitution. Thus because of decrease in oxidation state due to fluorine doping we can say that more  $Mn^{3+}$  with large ionic radii replace  $Mn^{4+}$ , increasing electrochemical performance. The initial capacity decay is due to strong Li-F bond which hinders the lithium extraction leads to low reversible capacity. Cycling performance increases due to strong M-F bond. Also helps in reduction of impedance.

#### **Why Mg is so important:**

- (i) The doped Mg will block the tetrahedral sites which is the path for transition metal ions to migrate from transition metal to lithium layer.
- (ii) Due to high ionic radii of magnesium, unit cell volume increases, this restricts the movement of TM ions.
- (iii) Also the ionic radii of  $Mg^{2+}$  (0.72Å) is close to  $Li^+$  (0.76Å) so it is possible to place  $Mg^{2+}$  in lithium sites. Thus structure transformation can be mitigated by Mg doping as Mg replace Ni during cycling.

## 2.4 Experimentation

### 2.4.1 Material preparation- Mg and F doped LMR-NMC

$\text{Li}_{1.2}\text{Mn}_{0.55}\text{Mg}_{0.01}\text{Ni}_{0.14}\text{Co}_{0.10}\text{O}_2$  was prepared by combustion synthesis. The precursors used in synthesis are lithium nitrate ( $\text{LiNO}_3$ ), manganese nitrate ( $\text{Mn}(\text{NO}_3)_2$ ), magnesium nitrate ( $\text{Mg}(\text{NO}_3)_2$ ), nickel nitrate ( $\text{Ni}(\text{NO}_3)_2$ ), cobalt nitrate ( $\text{Co}(\text{NO}_3)_2$ ) and Glycine. The stoichiometric amount of precursors were dissolved in an appropriate quantity of distilled water. The solution was heated at  $110^\circ\text{C}$  with continuous stirring until the solution turned into a high viscous gel. The obtained gel was placed in a preheated muffle furnace which is at  $400^\circ\text{C}$ , auto-ignition takes place releasing the smoke and forming the metal oxide.

The obtained metal oxide (by combustion synthesis) was mixed with appropriate amount of LiF using mortar-pestle in stoichiometric ratio of 1:100 (LiF: Metal oxide). Finally the mixture was annealed at  $800^\circ\text{C}$  for 20h in muffle furnace.

Powder X-ray diffraction (X'Pert PRO PANalytical) using Cu-K $\alpha$  radiation was used to identify the crystalline phase of the as prepared powders. Rietveld refinement was then performed on the X-ray diffraction data to obtain the lattice parameter. The XRD spectra were collected in a range of  $2\theta$  values from  $10^\circ$  to  $90^\circ$  at a scanning rate of  $1^\circ$  per min and a step size of  $0.02^\circ$ . The morphologies of the as-synthesized samples were observed by scanning electron microscope (SEM, Carle Zeiss SUPRA 40TM).

The electrochemical properties of cathode material containing LMR-NMC as the active mass was measured using two electrodes Swage-lok cells with Li as counter electrode. The electrolyte consisted of 1 M  $\text{LiPF}_6$  in a mixture of ethylene methyl carbonate and ethylene carbonate at a 1:1 volume ratio. For fabrication of the cathodes, the prepared powders were mixed with carbon black and polyvinylidene fluoride (PVDF) (80:10:10) in N-methylpyrrolidinone (NMP). The obtained slurry was coated onto Al foil. The cells were assembled in an argon-filled glove box (MBRAUN). The galvanostatic charge–discharge tests and cyclic voltammetry were carried out on a battery measurement system (ARBIN INSTRUMENTS) within a voltage range of 2.5–4.65 V vs.  $\text{Li}/\text{Li}^+$  at room temperature ( $25^\circ\text{C}$ ). Electrochemical impedance spectroscopy (EIS) measurements of all the samples were conducted at open circuit voltage in the frequency range of 1 MHz to 10 mHz with an amplitude of 5 mV using an electrochemical impedance analyzer (Solartron Analytical FRA1470E).

## 2.4.2 Structural and morphological characterization techniques:

All the synthesized materials were characterized by various characterization techniques such as XRD (X-Ray Diffraction), SEM (Scanning Electron Microscopy), and EDX map. SEM (scanning electron microscopy) was utilized to examine the morphology. EDX was done to measure the elemental composition of synthesized materials.

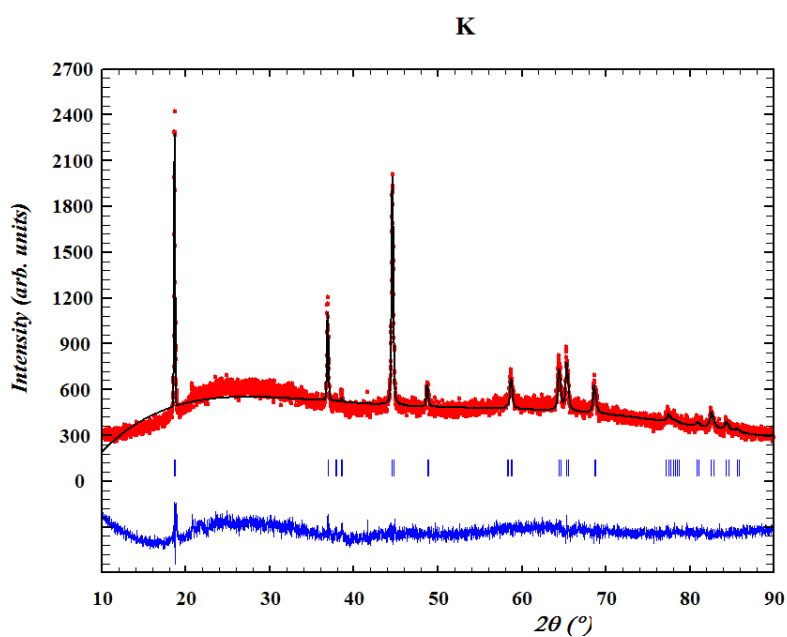


Fig. 2.4. (a) XRD of LMR-NMC.

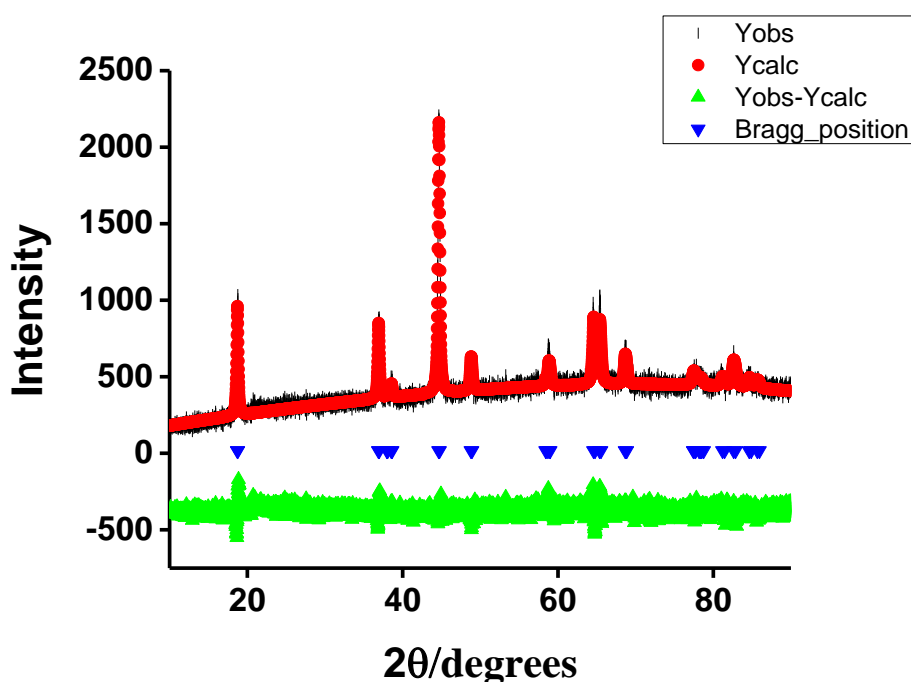


Fig. 2.4 (b) XRD of Mg-F Doped LMR-NMC ( $\text{Li}_{1.2}\text{Ni}_{0.14}\text{Mn}_{0.55}\text{Co}_{0.102}\text{Mg}_{0.01}\text{O}_{2-x}\text{F}_x$ )



Lattice parameters obtained by Rietveld refinement for LMR-NMC and Mg-F doped LMR-NMC are as follows:

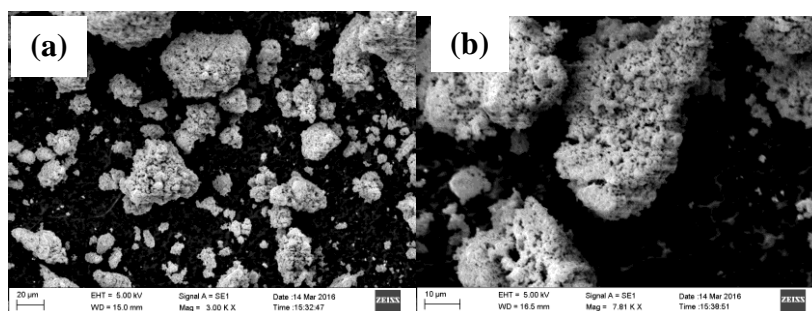
	A	b	c
LMR-NMC	2.8539 Å	2.8539 Å	14.2521 Å.
Mg-F LMR-NMC	2.8599 Å	2.8599 Å	14.2914 Å

**Table.2:** Rietveld refinement of LMR-NMC and Mg-F doped LMR-NMC

The crystal structure of LMR-NMC and Mg and F doped LMR-NMC were investigated by XRD. Each material is index to hexagonal crystal system  $\alpha$ -NaFeO<sub>2</sub>.

The minor peaks appearing at  $2\theta$  from  $21^\circ$  to  $23^\circ$  indicates the signature peak for lithium rich material, due to Li<sub>2</sub>MnO<sub>3</sub> (monoclinic) phase<sup>42</sup>. For both the samples lattice parameter was calculated from XRD spectrum. According to hexagonal crystal system the defined parameters ‘a’ and ‘c’ signify the size of transition metal oxygen slab and the interspacing of transition metal layers. The ‘a’ parameter is the measure of average M-M (M=Li, Ni, Mn, Co) distance in basal plane of hexagonal structure. The values of a, and c increases from 2.8539, 14.2521 to 2.8599, 14.2914. The ratio of these increment from a, and c are 0.21% and 0.27% respectively. Thus on basis of these results it is clear that both Mg and F doping in LMR-NMC has enlarged the lattice parameter of crystal structure, due to increase in both cell parameters (a and c). This may be due to partial reduction of TM ions by fluorine doping, also due to length of Mg-O bonding in layered oxide in larger than that of Ni-O.

The result obtained from Reiteveld refinement reveal that introduction of Mg and F neither affect the crystalline structure of precursor nor produce unwanted secondary phases. This result indicate that Mg and F have been completely introduced into crystal lattice of LMR-NMC.



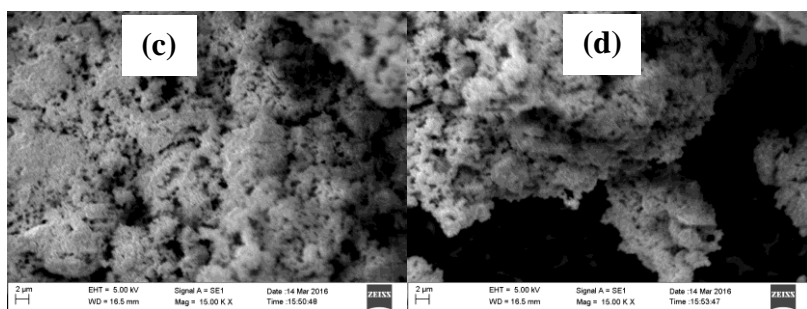


**Fig 2.5.** SEM Images of LMR-NMC (a)(b) , SEM Images of Mg-F Doped LMR-NMC (c)(d)

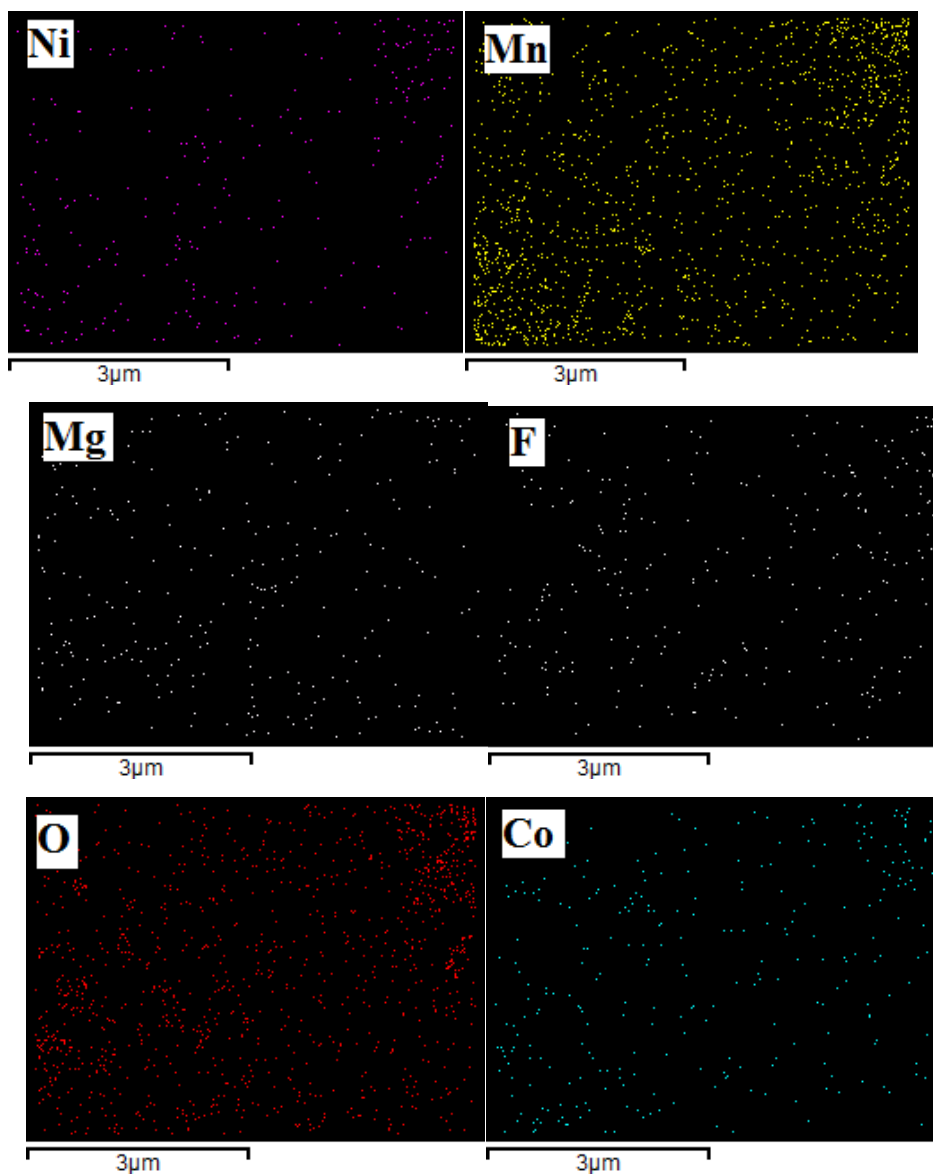


**Fig. 2.6.** EDX Characterizations of Mg-F Doped LMR-NMC Showing Ni, Mn, Mg, F, O and Co.

SEM images of LMR-NMC and Mg-F doped LMR-NMC are shown in e Fig.2.5 (a)-(d). Both Pristine and doped samples show similar morphology, with size of agglomerate about 20 $\mu$ m. From elemental mapping (**Fig. 2.6**) it is confirmed that all elements are distributed uniformly throughout the material and F and Mg are doped successfully.

### 2.4.3 Electrochemical Impedance Spectroscopy (EIS) studies:

EIS is a powerful technology provides the useful information about electrode resistance, reactance associated with electrochemical transport of the cell. EIS spectra of Mg and F doped LMR-NMC and pristine LMR-NMC are shown in Fig 2.6. The EIS spectra were interpreted during full charge condition in 10<sup>th</sup> cycle. For LMR-NMC the EIS data over full SOC range is complicated due to some factors which are- (i) due to activation of Li<sub>2</sub>MnO<sub>3</sub> phase at 4.5V, change in crystallographic phase (ii) continuous voltage fade during cycling represent bulk structural transition (iii) formation of SEI due to electrolyte decomposition at high voltage.

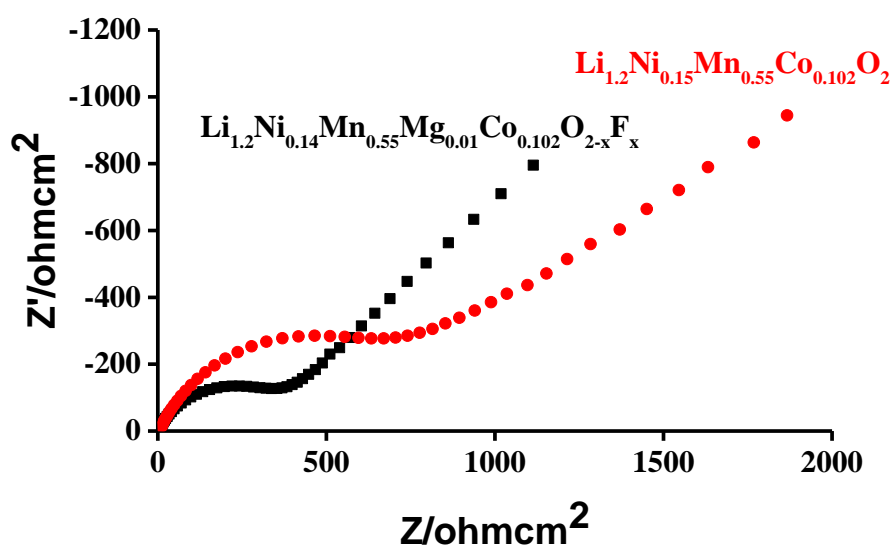


**Fig. 2.7.** Impedance Spectra of 10<sup>th</sup> Cycle, represented as Nyquist plots, of LMR-NMC & Mg-F doped LMR-NMC

All the Nyquist plots of Li<sub>1.2</sub>Ni<sub>0.14</sub>Mn<sub>0.55</sub>Co<sub>0.10</sub>Mg<sub>0.01</sub>O<sub>2-x</sub>F<sub>x</sub> and pristine LMR-NMC in **Fig. 2.7** are composed of two depressed semicircles and a slope. In high frequency region, the first semicircle is associated with surface film resistance ( $R_f$ ) formed by decomposition of

electrolyte on the surface of electrode during high voltage operation  $>4.5$  V. This semicircle represents Li ion diffusion in SEI. The second semicircle in middle frequency region is associated with charge transfer resistance ( $R_{ct}$ ) between SEI and active cathode material due to Li insertion reaction. The slope in low frequency region is associated with diffusion controlled process of Li ion in bulk. In impedance spectrum  $R_f$  falls at high frequency sometimes very small and overlap with  $R_{ct}$  if cell is not cycled. This may be due to the fact that  $R_f$  associated with SEI formation which is triggered largely by cycling. The impedance was taken for 10<sup>th</sup> cycle so there is very less SEI contribution. Thus the semicircle is largely due to charge transfer resistance ( $R_{ct}$ ) for both the samples due to charge transfer resistance ( $R_{ct}$ ) for both the samples.

Incorporation of Mg and F into material has decreased the electrode impedance and LiF coating on material decreases the polarization. The charge transfer resistance **Fig. 2.7** (for 10<sup>th</sup> cycle) is lower for doped LMR-NMC ( $\sim 383\Omega$ ) electrode compared to pristine LMR-NMC ( $\sim 710\Omega$ ) indicating improved rate and cycle life performance.

#### 2.4.4 Electrochemical Performance:

- i. Mg-F doped LMR-NMC shows high initial capacity,  $\sim 300$  mAh/g and that of pristine LMR-NMC is  $\sim 250$  mAh/g during 1<sup>st</sup> cycle.

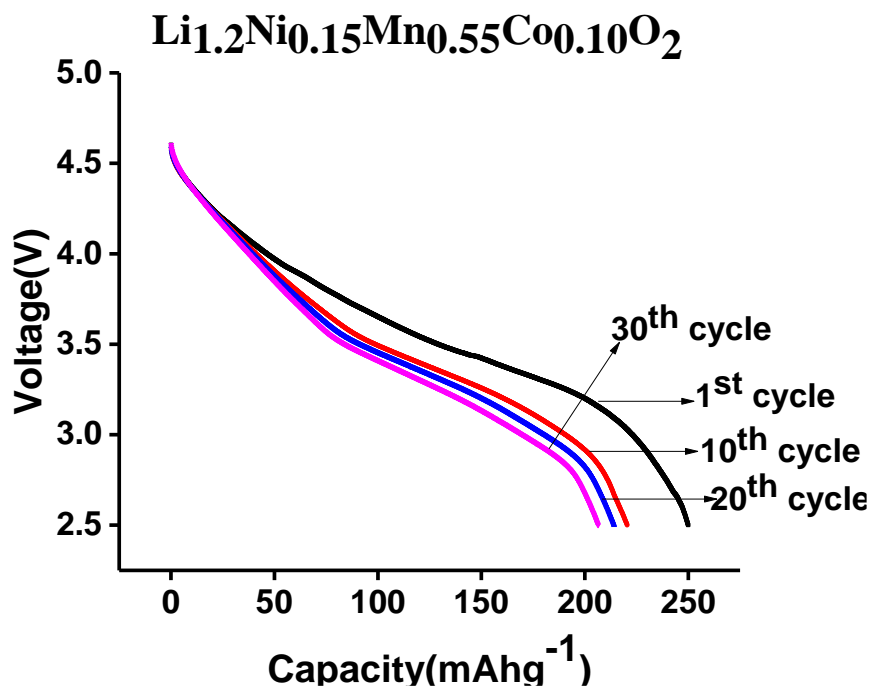


**Fig. 2.8. (a)** Discharge Profile of LMR-NMC

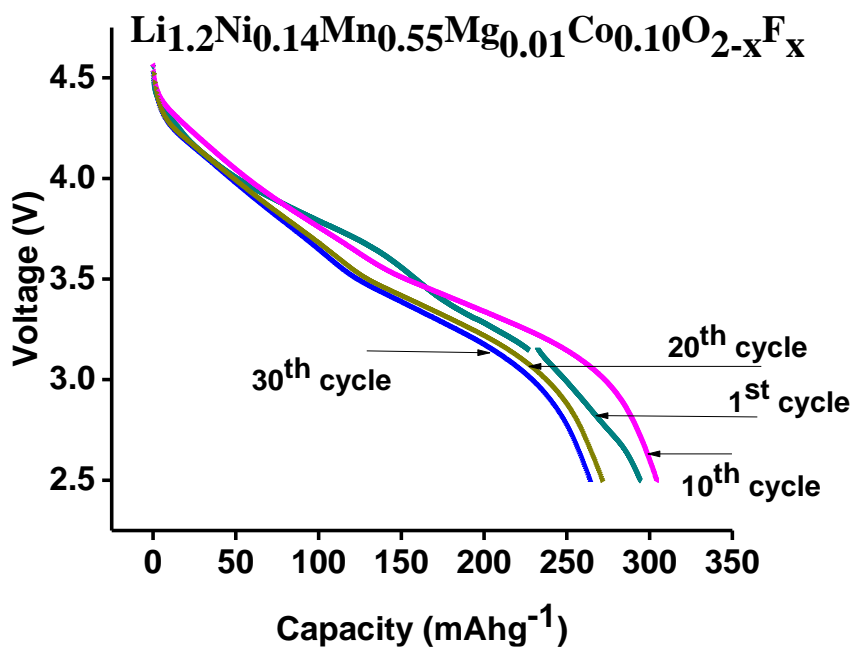


Fig. 2.8 (b) Discharge Profile of Mg-F Doped LMR-NMC

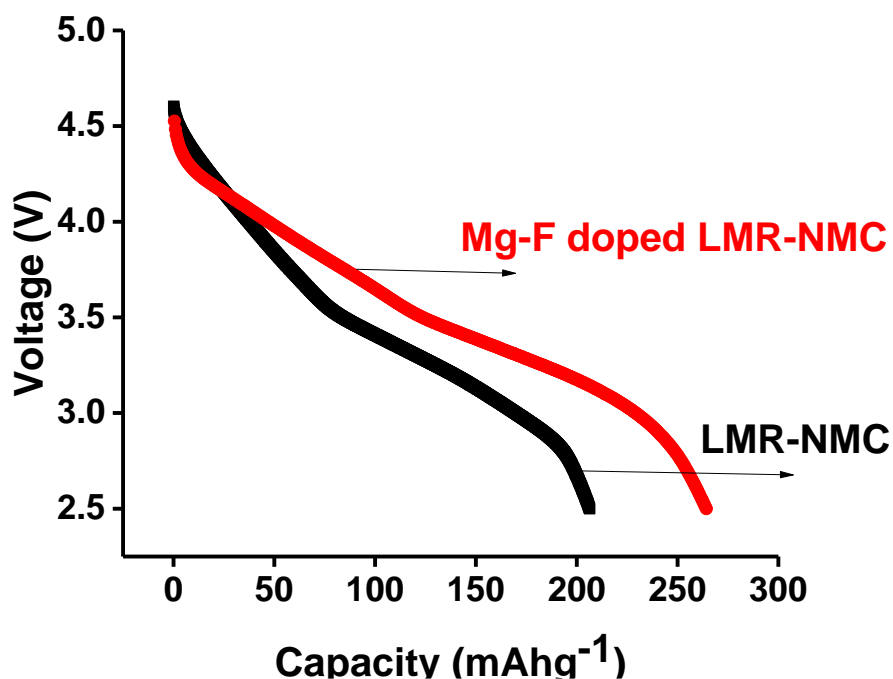


Fig. 2.8 (c) Discharge Profile of Both LMR-NMC and Mg-F LMR-NMC for 30<sup>th</sup> cycle

- ii. The discharge capacity of Mg-F doped LMR-NMC is  $>260 \text{ mAh/g}$  at C/10 rate for 30<sup>th</sup> cycle and corresponding pristine LMR-NMC is  $200 \text{ mAh/g}$ .
- iii. (c) Voltage fade is less ( $>0.3\text{V}$ ) for Mg-F doped LMR-NMC compared to LMR-NMC (for 30<sup>th</sup> cycle).

The high capacity is attributed to extra lithium which is added in form of LiF in Mg-F doped LMR-NMC. Also the voltage fade is less in case of doped sample as compare to pristine LMR-NMC. Due to successful doping of both Mg and F, results in high capacity this is due to structure stabilization by doping. As Mg and F helps in decrease in voltage fade thus it is helping in minimizing the structure transformation from layered to spinel.

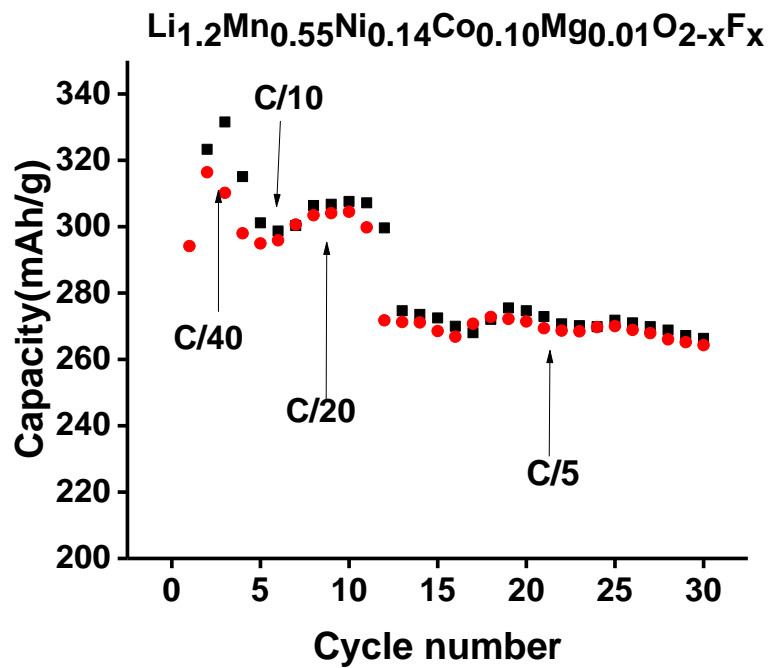


Fig.2.9 (a) Cycle Life Data of Mg-F doped LMR-NMC

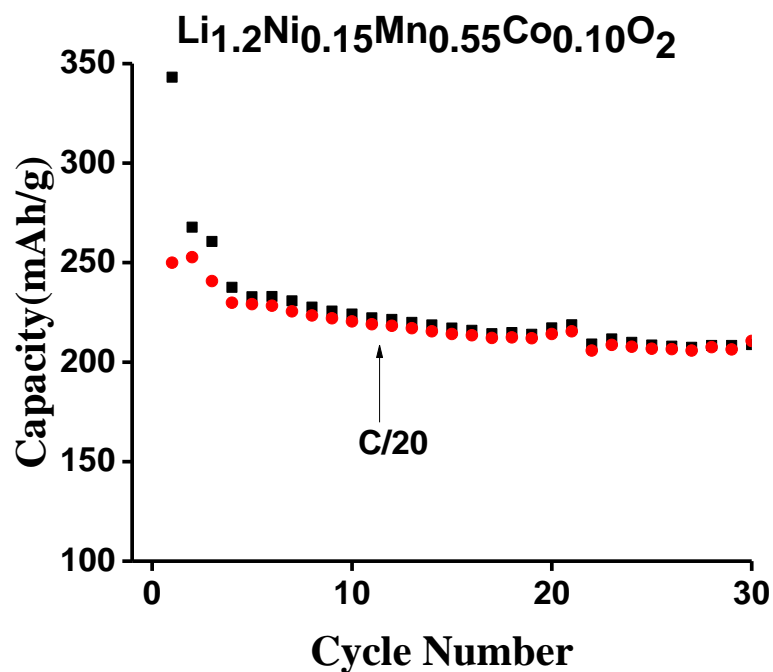
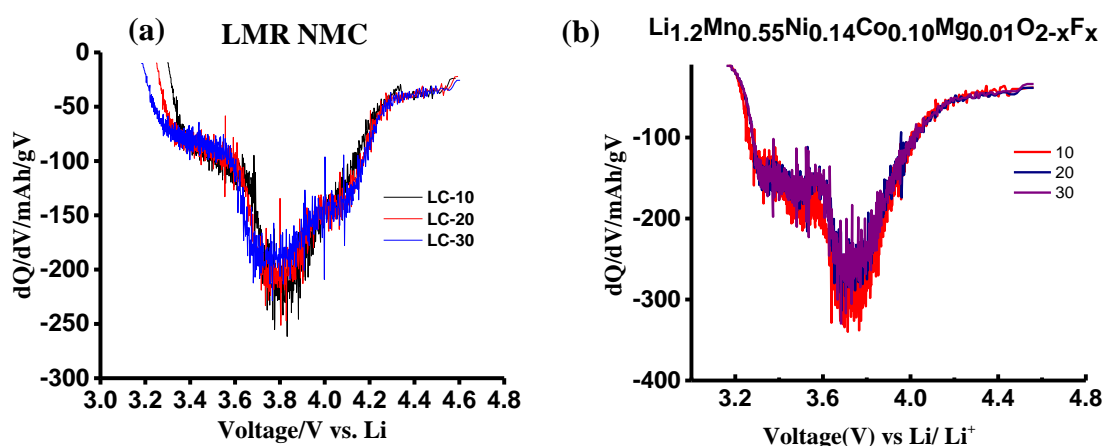


Fig.2.9 (b) Cycle Life Data of LMR-NMC

The cycling performance of material was tested between 2.5-4.65V at different C rates. **Fig 2.9(a), (b)** shows the comparison of cycling performance of both the samples. Mg and F doped LMR-NMC shows stable cycle life at different C rates ( $> 260 \text{ mAh g}^{-1}$  at C/5 rate), whereas pristine LMR NMC shows rapid capacity fade during cycling ( $200 \text{ mAh g}^{-1}$  at C/20 rate). The doped sample shows stable cycle life and stable capacity, almost no voltage decay indicating structural transition from layered to spinel have been mitigated to a certain extent.



**Fig 2.10.** dQ/dV Curves of Discharge Process for 10<sup>th</sup>, 20<sup>th</sup> & 30<sup>th</sup> cycle of (a) LMR-NMC  
(b) Mg-F Doped LMR-NMC

**Fig2.10** compare the dQ/dV curves for LMR-NMC and Mg-F doped LMR-NMC. Mg-F doped LMR-NMC shows stable voltage profile during cycling, indicates minimized voltage decay. dQ/dV curve of LMR-NMC moves towards lower voltage indicating voltage decay (structural transformation) during cycling for pristine LMR-NMC.

## 2.5 Conclusion:

- 1) Mg & F doped LMR-NMC is synthesized by solution combustion followed by solid state synthesis.
- 2) Increase in 'a' lattice parameter shows successful substitution of Ni<sup>2+</sup> by Mg<sup>2+</sup> lattice without change in crystal system.
- 3) The Mg and F doped LMR-NMC provides high capacity ( $\sim 300 \text{ mAh/g}$  at C/40 rate,  $\sim 260 \text{ mAh/g}$  at C/5 rate, stable cycle life and a stable voltage profile during cycling.
- 4) The EIS study of Mg & F doped LMR-NMC shows lower charge transfer resistance amounting to lower electrode impedance.

- 5) The enhanced electrochemical properties of the material can be related to the addition of Mg and F, which can effectively mitigate the structural deterioration during cycling.

## References

1. M. M. Thackeray, C. S. Johnson, J. T. Vaughey, N. Li and S. A. Hackney, *J. Mater. Chem.*, 2005, **15**, 2257.
2. M. N. Ates, Q. Jia, A. Shah, A. Busnaina, S. Mukerjee and K. M. Abraham, *J. Electrochem. Soc.*, 2014, **161**, A290.
3. C. S. Johnson, J. T. Vaughey and M. M. Thackeray, *Chem. Mater.*, 2008, **20**, 6095.
4. K. Jarvis, Z. Deng, L. Allard, A. Manthiram and P. Ferreira, *Microsc. Microanal.* 2011, **17**, 1578.
5. C. S. Johnson, S. D. Korte and J. T. Vaughey, et al., *J. Power Sources*, 1999, **491**, 81.
6. G. Yang, H. Ji, P. Gao, A. Hong, H. Ding, S. Roy, J. Pinto and X. Jiang, *J. Electrochem. Soc.*, 2011, **158**, A1071.
7. J. Jiang and J. R. Dahn, *Electrochim. Acta*, 2006, **51**, 3413.
8. M.M. Thackeray, C.S. Johnson, J.T. Vaughey, N. Li, S.A. Hackney, *J. Mater. Chem.*, 2006, **15** 2257.
9. B. Xu, C.R. Fell, M. Chi, Y.S. Meng, *Energy Environ. Sci.*, 2011, **4**, 2223.
10. V. Etacheri, R. Marom, R. Elazari, G. Salitra and D. Aurbach, *Energy Environ. Sci.*, 2011, **4**, 3243.
11. M. S. Whittingham, *Chem. Rev.*, 2004, **104**, 4271.
12. K. Kang, Y. S. Meng, J. Bréger, C. P. Grey and G. Ceder, *Science*, 2006, **311**, 977.
13. Y.-J. Kim, Y. Hong, M. G. Kim and J. Cho, *Electrochem. Commun.*, 2007, **9**, 1041.
14. B. Song, Z. Liu, M. Lai and L. Lu, *Phys. Chem. Chem. Phys.*, 2012, **14**, 12875.
15. L. Yu, W. Qiu, F. Lian, J. Huang and X. Kang, *J. Alloys Compd.*, 2009, **471**, 317.
16. Y. Wu and A. Manthiram, *Electrochem. Solid-State Lett.*, 2007, **10**, A151.
17. Y. Koyama, I. Tanaka, M. Nagao and R. Kanno, *J. Power Sources*, 2009, **189**, 798.
18. L. Yu, W. Qiu, F. Lian, J. Huang and X. Kang, *J. Alloys Compd.*, 2009, **471**, 317.
19. Z. Q. Deng and A. Manthiram, *J. Phys. Chem. C* 2011, **115**, 7097.
20. Z. H. Lu and J. R. Dahn, *J. Electrochem. Soc.*, 2002, **149**, A815.
21. Denis, Y.; Yanagida, K., *J. Electrochem. Soc.* 2011, **158**, A1015.
22. Y.K. Sun, M.J. Lee, C. S. Yoon, J. Hassoun, K. Amine and B. Scrosati, *Adv. Mater.*, 2012, **24**, 1192.



23. Y. Wu and A. Manthiram, *Solid State Ionics*, 2009, **180**, 50.
24. Z. Wang, E. Liu, C. He, C. Shi, J. Li and N. Zhao, *J. Power Sources*, 2013, **236**, 25.
25. W. C. West, J. Soler, M. C. Smart, B. V. Ratnakumar, S. Firdosy, V. Ravi, M. S. Anderson, J. Hrbacek, E. S. Lee and A. Manthiram, *J. Electrochem. Soc.*, 2011, **158**, A883.
26. B. Liu, Q. Zhang, S. He, Y. Sato, J. Zheng, *Electrochim. Acta*, 2011, **56**, 6748.
27. W. Liu, P. Oh, X. Liu, M.-J. Lee, W. Cho, S. Chae, Y. Kim and J. Cho, *Angew. Chem., Int. Ed.*, 2015, **54**, 4440.
28. K. M. Shaju and P. G. Bruce, *J. Power Sources*, 2007, **174**, 1201.
29. Z. Tang, Z. Wang, X. Li and W. Peng, *J. Power Sources*, 2012, **204**, 187.
30. M. Tabuchi, Y. Nabeshimaa, T. Takeuchia, H. Kageyamaa, K. Tatsumia, J. Akimotob, H. Shibuyac and J. Imaizumi, *J Power Sources*, 2011, **196**, 3611.
31. M. Tabuchi, Y. Nabeshima, T. Takeuchi, H. Kageyama, J. Imaizumi, H. Shibuya and J. Akimoto, *J. Power Sources*, 2013, **221**, 427.
32. L. Jiao, M. Zhang, H. Yuan, M. Zhao, J. Guo, W. Wang, X. Zhou and Y. Wang, *J. Power Sources*, 2007, **167**, 178.
33. B. Song, M. Lai and L. Lu, *Electrochim. Acta*, 2012, **80**, 187.
34. Y. N. Ko, J.-H. Kim, J.-K. Lee, Y. C. Kanga and J.-H. Lee, *Electrochim. Acta*, 2012, **69**, 345.
35. Q. Liu, K. Du, G. Hu, Z. Peng, Y. Cao and W. Liu, *Solid State Ionics*, 2012, **23**, 227.
36. Xu, B.; Fell, C. R.; Chi, M.; Meng, Y. S, *Energy Environ. Sci.* 2011, **4**, 2223.
37. Wei He, Dingding Yuan, Jiangfeng Qian, Xinping Ai, Hanxi Yang and Yuliang Cao, *J. Mater. Chem. A*, 2013, **1**, 11397.
38. C. J. Jafta, K. I. Ozoemena, M. K. Mathe, and W. D. Roos, *Electrochim. Acta*, 2012, **85**, 411.
39. Qi Li, Guangshe Li, Chaochao Fu, Dong Luo, Jianming Fan, and Liping Li, *ACS Appl. Mater. Interfaces* 2014, **6**, 10330.
40. Wei He, Dingding Yuan, Jiangfeng Qian, Xinping Ai, Hanxi Yang and Yuliang Cao, *J. Mater. Chem. A*, 2013, **1**, 11397.
41. Mehmet Nurullah Ates, Qingying Jia, *J. Electrochem. Soc.*, 2014, **161** A290-A301.
42. Hongjie Xu, Shengnan Deng and Guohua Chen, *J. Mater. Chem. A*, 2014, **2**, 15015–15021.